

Millisecond Time-Scale Folding and Unfolding of DNA Hairpins Using Rapid-Mixing Stopped-Flow Kinetics

Rajesh K. Nayak,[†] Olve B. Peersen,[‡] Kathleen B. Hall,[§] and Alan Van Orden^{*,†}

[†]Department of Chemistry and [‡]Department of Biochemistry and Molecular Biology, Colorado State University, Fort Collins, Colorado 80523, United States

[§]Department of Biochemistry and Molecular Biophysics, Washington University School of Medicine, St. Louis, Missouri 63110, United States

S Supporting Information

ABSTRACT: We report stopped-flow kinetics experiments to study the folding and unfolding of 5 base-pair stem and 21 nucleotide polythymidine loop DNA hairpins over various concentrations of NaCl. The reactions occurred on a time scale of milliseconds, considerably longer than the microsecond time scale suggested by previous kinetics studies of similar-sized hairpins. In comparison to a recent fluorescence correlation spectroscopy study (*J. Am. Chem. Soc.* **2006**, *128*, 1240–1249), we suggest the microsecond time-scale reactions are due to intermediate states and the millisecond time-scale reactions reported here are due to the formation of the fully folded DNA hairpin. These results support our view that DNA hairpin folding occurs via a minimum three-state mechanism.

A clear understanding of the biomolecular structures and functions¹ of nucleic acids requires proper insight into how these molecules fold, unfold, and sometimes misfold.² DNA and RNA hairpins are important model systems for understanding the kinetics and thermodynamics of such processes.^{3–5} Consisting of a single-stranded loop and a base-paired stem, these molecules can undergo conformational fluctuations^{6–8} of the unfolded strand, loop formation, base-stacking,^{9–11} and intramolecular Watson–Crick and non-Watson–Crick base-pairing.¹² Hence, a variety of molecular processes in nucleic acids can be investigated by studying these hairpins.

The folding kinetics of DNA and RNA hairpins has been the subject of numerous experimental and theoretical investigations.^{9,13–17,23–25} Yet controversy remains concerning many aspects of the folding kinetics, including folding times, mechanisms, rate-limiting steps, and their dependence on sequence, loop size, stem size, salt concentration, temperature, etc.^{10,18–20} Smaller hairpins, containing up to 5 base-pairs (bp) in the stem and 4–30 nucleotides (nt) in the loop, have been examined using laser-induced temperature jump^{21,22} and fluorescence correlation spectroscopy (FCS) experiments.^{6,23–25} These studies reveal reaction times of ~10–100 μ s, depending on loop size and other conditions. Hairpins with longer stems have been studied using single-molecule optical trapping techniques,^{26,27} revealing much longer folding and

unfolding times of milliseconds to hundreds of milliseconds, depending on stem size.

Previously, our laboratory used FCS to study the folding and unfolding kinetics of DNA hairpins containing a 5-bp stem and 21-nt polythymidine loop under various conditions.²⁵ Reaction times of ~50 μ s were observed, consistent with previous studies of similar-sized hairpins. However, careful examination of the correlation amplitudes along with photon-counting histogram analysis revealed that the reaction being probed by our FCS experiment was likely due to an intermediate state in a more complex reaction mechanism. We hypothesized that the overall reaction involving the fully folded hairpin occurred on a longer time scale than the FCS observation time and was thus not observed in our experiment. A later study²³ that combined single-beam autocorrelation and two-beam cross-correlation spectroscopy observed the reactions of hairpins with 4-bp and 5-bp stem sizes on an extended time scale. This study revealed that the reaction time for complete folding of the 4-bp structure was ~400 μ s. Only the intermediate reaction of the 5-bp structure was observed, even with the expanded observation time. This implied that complete folding of the 5-bp stem length hairpin may occur on a millisecond time scale or longer.

Here, we report folding kinetics of the 5-bp stem size DNA hairpin on the millisecond time scale using the rapid-mixing stopped-flow technique.²⁸ Stopped-flow kinetics observes the time evolution of a reaction initiated by the mixing of two or more reagents. A drawback of this method is the finite mixing time, typically 0.5 ms or longer. Reactions that occur faster than the mixing time are not observed. Hence, the ~50 μ s reaction observed in our previous FCS experiments is inaccessible using stopped-flow. However, if the overall reaction occurs on a much longer time scale, as suggested previously, we hypothesized that stopped-flow may be an appropriate technique to measure its kinetics.

Figure 1 shows stopped-flow kinetics data obtained for 100 nM DNA hairpins in an aqueous buffer. The DNA hairpins consisted of a 5-bp stem containing the complementary sequences 5'-AACCC and GGGTT-3' connected by a 21-nt polythymidine loop. The DNA hairpin 5'-AACCC-(T)₂₁GGGTT-3' was labeled at the 5' end with tetramethylrhodamine (TAMRA) and at the 3' end with 4-(4-dimethylaminophenylazo) benzoic acid (dabcyl) quencher.

Received: September 8, 2011

Published: January 19, 2012

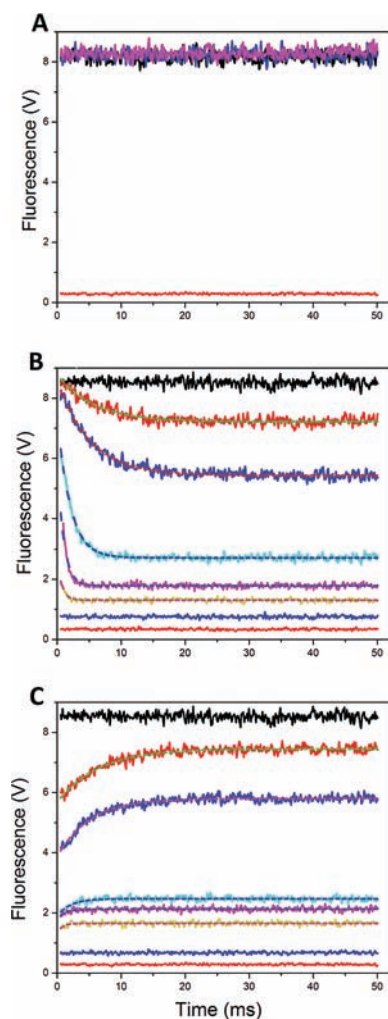


Figure 1. Experimental data (solid lines) and corresponding fitting curves (solid dashed lines) from stopped-flow measurements of (A) folding reaction of control DNA for comparison, (B) DNA hairpin hp(T)₂₁ folding reaction, and (C) DNA hairpin unfolding reaction as a function of varying NaCl concentration (black, 0; red, 5; blue, 10; dark cyan, 25; magenta, 50; dark yellow, 100; and navy, 500 mM NaCl; wine, background buffer).

The folding of the DNA hairpin, induced by mixing the DNA with buffer solutions containing varying concentrations of NaCl, was monitored by observing the quenching of the TAMRA fluorophores by dabcyf (Figure 1B) after a mixing time of $\sim 450 \mu\text{s}$. Unfolding was monitored by observing the recovery of the fluorescence due to mixing DNA solutions containing varying concentrations of NaCl with pure buffer (Figure 1C). All experiments were carried out at a laboratory temperature of $\sim 22^\circ\text{C}$. Because DNA is a polyanion, Na^+ counterions are necessary to stabilize the hairpin in its folded state. Hence, mixing the DNA with NaCl induced the formation of the hairpin, whereas mixing with pure buffer caused the hairpins to dissociate. The reaction rates increased with increasing NaCl concentration. The same mixing experiments were carried out for a control DNA sample containing a TAMRA fluorophore in the absence of quencher (Figure 1A). These latter experiments demonstrate that NaCl does not affect the intensity of the TAMRA dye fluorescence. Control experiments using zero concentration NaCl (black curves) and blank buffer solutions (red curves) are also shown for

comparison. Thermodynamic analysis ruled out the possibility of duplex and/or quadruplex formation interfering with the stopped-flow kinetics data under our experimental conditions (see Supporting Information).

To estimate the reaction times of the DNA hairpin folding and unfolding reactions, we fit the data shown in Figure 1 to single-exponential functions (solid curves). The reaction times decreased with NaCl concentration, ranging from 6.38 ms for 5 mM NaCl to 0.77 ms for 100 mM NaCl (see Table 1, below).

Table 1. Kinetic Parameters of DNA Hairpin hp(T)₂₁ at Different NaCl Concentrations (Considering Two-State Model)^a

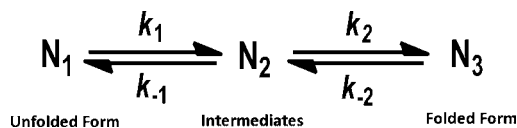
[NaCl] (mM)	K_{melt}	τ_{rxn} (ms)
5	0.60	6.38(0.18)
10	1.20	5.05(0.13)
25	3.94	2.08(0.19)
50	9.09	1.33(0.29)
100	21.21	0.77(0.23)

^a τ_{rxn} corresponds to the fitting analysis in Figure 1 B,C, and K_{melt} is determined from melting curve analysis (Supporting Information). Numbers in parentheses are uncertainties in the last digits.

Table 1 also shows the apparent equilibrium constant, $K_{\text{melt}} = [\text{folded}]/[\text{unfolded}]$, obtained from analysis of the melting curves assuming a two-state reaction process (see Supporting Information). Within experimental error, the reaction times were identical for folding and unfolding experiments with the same NaCl concentration. For the 500 mM NaCl sample, the folding reaction occurred during the stopped-flow mixing time. Importantly, the reaction times reported here are approximately an order of magnitude longer than those reported in previous kinetics studies on similar-sized hairpins.^{6,12,18,23–25}

To investigate the relationship between the stopped-flow kinetics experiments reported here and the FCS experiments reported previously, we analyzed our stopped-flow data using the three-state mechanism proposed in our previous FCS study (Scheme 1).²⁵

Scheme 1. Proposed Kinetic Mechanism for DNA Hairpin Folding/Unfolding Reactions



The Supporting Information section shows the rate equations used to predict the fluorescence decay under initial conditions given by (N_1, N_2, N_3) equal to $(N_{\text{total}}, 0, 0)$. The fluorescence decay is assumed to be proportional to the decay of the N_1 concentration over time. This, in turn, depends on the total DNA concentration and the rate constants, k_1 , k_{-1} , k_2 , and k_{-2} . The rate constants k_1 , k_{-1} for DNA hairpins in 100 mM NaCl were determined in our previous FCS study.²⁵ Figure 2 shows the result of fitting our stopped-flow data for the DNA hairpin in 100 mM NaCl to the three-state mechanism. k_1 and k_{-1} were constrained to the values determined by FCS,²⁵ and the initial fluorescence was constrained to the fluorescence observed from the control sample in the absence of quencher. k_2 and k_{-2} were adjustable parameters in the fit. A fit to a two-state mechanism with the initial fluorescence constrained is also

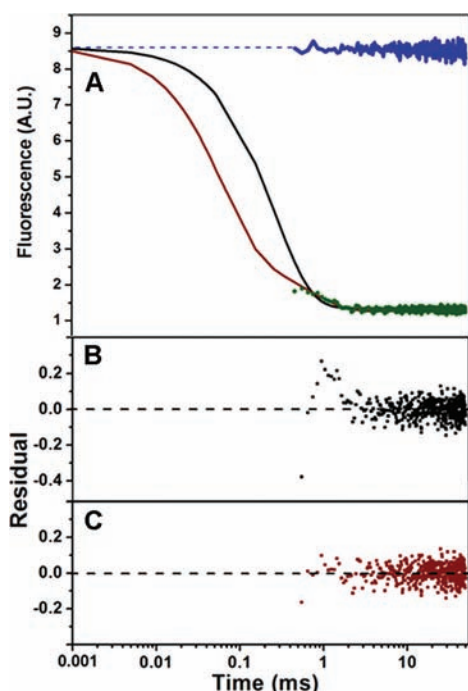


Figure 2. (A) Stopped-flow kinetics data for DNA hairpins in 100 mM NaCl (green dots) and fitting curves to a two-state (black) and three-state (wine) mechanism. The blue curve shows the stopped-flow data of a control DNA hairpin in the absence of quencher. (B) Residual plot for the two-state mechanism. (C) Residual plot for the three-state mechanism.

shown for comparison. By plotting the data on a semilog scale, it is easily seen that the bulk of the reaction occurs during the stopped-flow mixing time. In particular, the three-state mechanism predicts a two-phase decay process, with the initial phase going to completion before the mixing is complete. Nevertheless, it is clear from the fitting curves and the residual plots in Figure 2 that the stopped-flow data observed after the mixing time fit well to the three-state mechanism but do not fit to the two-state mechanism. Hence, the stopped-flow data reported here are consistent with the three-state mechanism discussed previously for the 100 mM NaCl sample. Note that the single-exponential fits displayed in Figure 1 fit the data well because the intensities were not constrained.

Table 2 shows the parameters of the three-state mechanism based on the present stopped-flow kinetics data and previous FCS data for DNA hairpin folding in 100 mM NaCl. Also shown are the reaction time constants, $1/\tau_{\text{rxn}1,2} = k_{1,2} + k_{-1,-2}$

Table 2. Kinetic Parameters of DNA Hairpin hp(T)₂₁ in 100 mM NaCl Buffer^a

parameter	previous work ²⁵	present work
$\tau_{\text{rxn}1}$ (μs)	62.7 (5.1)	–
k_1 (s^{-1})	$(1.12 \pm 0.16) \times 10^4$	–
k_{-1} (s^{-1})	$(4.79 \pm 0.050) \times 10^3$	–
$\tau_{\text{rxn}2}$ (μs)	–	472(± 13)
k_2 (s^{-1})	–	$(1.39 \pm 0.26) \times 10^3$
k_{-2} (s^{-1})	–	$(0.73 \pm 0.08) \times 10^3$
K_1	2.33(0.22)	–
K_2	4.75(0.33)	1.91(± 0.19)
K_{overall}	8.35(1.20)	4.47(± 0.85)

^aNumbers in parentheses are the uncertainties in the last digits.

and equilibrium constants $K_1 = k_1/k_{-1}$, $K_2 = k_2/k_{-2}$, and $K_{\text{overall}} = K_1K_2$. The latter constants, K_2 and K_{overall} , are in reasonable agreement with those deduced from our previous FCS study.²⁵ Note that the equilibrium constant K_{overall} should not be compared to the constant K_{melt} shown in Table 1, as this latter constant was obtained from melting curve analysis assuming a two-state reaction mechanism (see Supporting Information). In our previous FCS study,²⁵ we showed that the observed melting profile of the DNA hairpins could be reproduced from the proposed three-state mechanism, but the overall equilibrium constant derived from these curves differed depending on the chosen mechanism. The reaction time constants reported here confirm that the overall DNA hairpin folding reaction occurs on a time scale that is significantly longer than previous kinetics studies suggest. It is concluded that the DNA hairpin folding reaction in 100 mM NaCl is a complex process that occurs over a broad time range and must be examined using complementary experimental techniques sensitive to disparate time scales.

The DNA hairpin folding reactions in 25 and 50 mM NaCl can also be explained using a three-state reaction mechanism. However, complete analysis of the stopped-flow data for these samples awaits more careful FCS measurements of the k_1 and k_{-1} rate constants than reported in our previous FCS studies.²⁵ By contrast, the reactions occurring in 5 and 10 mM NaCl do not appear to fit the three-state mechanism. Rather, the reactions in these samples can be best described as reversible two-state processes with single-exponential decay. These results are similar to our previous FCS study, which found the reactions in NaCl below 25 mM were predominantly two-state reactions.²⁵ The three-state mechanism was used to explain reactions at higher NaCl concentrations. However, in the previous study, it was assumed the two-state reactions at low NaCl concentration involved the folding and unfolding of the intermediate state. By contrast, the present study suggests a direct folding and unfolding reaction involving the unfolded state and the folded DNA hairpin at low NaCl concentration. Our interpretation of the stopped-flow kinetics data reported here and the FCS data reported previously²⁵ is as follows. At low NaCl concentration, the DNA hairpin folding reaction occurs as a slow, reversible, two-state process involving direct folding and unfolding of the folded state. As the NaCl concentration increases, the reaction becomes faster, and intermediate forms of the DNA hairpin begin to stabilize. At higher NaCl concentration, the reaction proceeds according to a three-state mechanism involving stable or metastable intermediates.

Several theoretical studies using statistical mechanics and molecular dynamics models have examined the intermediate forms of RNA and DNA hairpins.^{10,14,19,20} Chen and co-workers used statistical mechanics modeling²⁰ to investigate the role of these intermediates on the reaction rates and mechanism. Several types of intermediate states were identified that involve partial folding of the stem and/or mismatched Watson–Crick and non-Watson–Crick base-pairing in the stem and loop. Formation and disruption of off-path intermediates can serve as the rate-limiting step of the reaction, whereas on-path intermediates can increase the rate compared to a direct two-state mechanism. We suggest the changes in rate and mechanism we observed with NaCl concentration may be due to the role of Na⁺ counterions in stabilizing various intermediate forms of the DNA hairpin.

In summary, we have reported stopped-flow kinetics experiments to investigate the folding and unfolding kinetics of a DNA hairpin molecule. The observed reactions were found to occur on a millisecond time scale, suggesting DNA hairpin formation can occur much more slowly than previously thought. We suggest a three-state reaction mechanism, wherein intermediate formation occurs on a tens to hundreds of microseconds time scale, and complete hairpin formation occurs on a millisecond time scale. FCS is useful for probing the intermediate reactions, but cannot observe the complete folding reaction due to the limited observation time of FCS. Likewise, stopped-flow can observe the complete folding reaction but cannot observe the intermediate reaction due to the finite dead time. When combined with each other, these techniques can monitor the complete folding trajectory of the DNA hairpin.

■ ASSOCIATED CONTENT

■ Supporting Information

Experimental procedures for stopped-flow, steady-state measurements, derivation for three-state models, and detailed thermodynamic analysis of hairpin formation. This material is available free of charge via the Internet at <http://pubs.acs.org>.

■ AUTHOR INFORMATION

Corresponding Author

vanorden@lamar.colostate.edu

Notes

The authors declare no competing financial interest.

■ ACKNOWLEDGMENTS

This research was supported by an ARRA supplement to NIH grant no. GM077231 (K.B.H.) and NSF grant 0920588 (A.V.O.). We thank Branka Ladanyi, Peng Gong, Artem Melnykov, and P. B. Chatterjee for helpful discussions.

■ REFERENCES

- (1) Hall, K. B. *Curr. Opin. Chem. Biol.* **2008**, *12*, 612.
- (2) Dobson, C. M. *Nature* **2003**, *426*, 884.
- (3) Bevilacqua, P. C.; Blose, J. M. *Annu. Rev. Phys. Chem.* **2008**, *59*, 79.
- (4) Chen, S. J. *Annu. Rev. Biophys.* **2008**, *37*, 197.
- (5) Woodside, M. T.; Anthony, P. C.; Behnke-Parks, W. M.; Larizadeh, K.; Herschlag, D.; Block, S. M. *Science* **2006**, *314*, 1001.
- (6) Bonnet, G.; Krichevsky, O.; Libchaber, A. *Proc. Natl. Acad. Sci. U.S.A.* **1998**, *95*, 8602.
- (7) Volker, J.; Makube, N.; Plum, G. E.; Klump, H. H.; Breslauer, K. J. *Proc. Natl. Acad. Sci. U.S.A.* **2002**, *99*, 14700.
- (8) Wallace, M. I.; Ying, L.; Balasubramanian, S.; Klenerman, D. *Proc. Natl. Acad. Sci. U.S.A.* **2001**, *98*, 5584.
- (9) Grunwell, J. R.; Glass, J. L.; Lacoste, T. D.; Deniz, A. A.; Chemla, D. S.; Schultz, P. G. *J. Am. Chem. Soc.* **2001**, *123*, 4295.
- (10) Tan, Z.-J.; Chen, S.-J. *Biophys. J.* **2008**, *95*, 738.
- (11) Zhang, W.; Chen, S. J. *Proc. Natl. Acad. Sci. U.S.A.* **2002**, *99*, 1931.
- (12) Ansari, A.; Kuznetsov, S. V.; Shen, Y. *Proc. Natl. Acad. Sci. U.S.A.* **2001**, *98*, 7771.
- (13) Liphardt, J.; Onoa, B.; Smith, S. B.; Tinoco, I.; Bustamante, C. *Science* **2001**, *292*, 733.
- (14) Portella, G.; Orozco, M. *Angew. Chem.* **2010**, *122*, 7839.
- (15) Van Orden, A.; Jung, J. *Biopolymers* **2008**, *89*, 1.
- (16) Werner, J. H.; Joggerst, R.; Dyer, R. B.; Goodwin, P. M. *Proc. Natl. Acad. Sci. U.S.A.* **2006**, *103*, 11130.
- (17) Yin, Y.; Zhao, X. S. *Acc. Chem. Res.* **2011**, *19*, 12799.

- (18) Ansari, A.; Shen, Y.; Kuznetsov, S. V. *Phys. Rev. Lett.* **2002**, *88*, 069801.
- (19) Sorin, E. J.; Engelhardt, M. A.; Herschlag, D.; Pande, V. S. *J. Mol. Biol.* **2002**, *317*, 493.
- (20) Zhang, W.; Chen, S.-J. *Biophys. J.* **2006**, *90*, 778.
- (21) Ma, H.; Proctor, D. J.; Kierzek, E.; Kierzek, R.; Bevilacqua, P. C.; Gruebele, M. *J. Am. Chem. Soc.* **2006**, *128*, 1523.
- (22) Ma, H.; Wan, C.; Wu, A.; Zewail, A. H. *Proc. Natl. Acad. Sci. U.S.A.* **2007**, *104*, 712.
- (23) Jung, J.; Ihly, R.; Scott, E.; Yu, M.; Van Orden, A. *J. Phys. Chem. B* **2008**, *112*, 127.
- (24) Jung, J.; Van Orden, A. *J. Phys. Chem. B* **2005**, *109*, 3648.
- (25) Jung, J.; Van Orden, A. *J. Am. Chem. Soc.* **2006**, *128*, 1240.
- (26) Gupta, A. N.; Vincent, A.; Neupane, K.; Yu, H.; Wang, F.; Woodside, M. T. *Nat. Phys.* **2011**, *7*, 631.
- (27) Woodside, M. T.; Behnke-Parks, W. M.; Larizadeh, K.; Travers, K.; Herschlag, D.; Block, S. M. *Proc. Natl. Acad. Sci. U.S.A.* **2006**, *103*, 6190.
- (28) Gong, P.; Campagnola, G.; Peersen, O. B. *Anal. Biochem.* **2009**, *391*, 45.